

Condensation and evaporation on a randomly occupied square lattice

Tapati Dutta,¹ Nikolai Lebovka,² and S. Tarafdar^{3,*}

¹ *Physics Department, St Xavier's College, Kolkata 700016, India*

² *Biocolloid Chemistry Institute, 42, Vernadsky Avenue, Kyiv, Ukraine*

³ *Condensed Matter Physics Research Centre, Physics Department, Jadavpur University, Kolkata 700032, India*

(Received 17 May 2002; published 10 October 2002)

We study the evolution of an initially random distribution of particles on a square lattice, under certain rules for “growing” and “culling” of particles. In one version we allow the particles to move laterally along the surface (mobile layer) and in the other version this motion is not allowed (immobile case). In the former case, both analytical and computer simulation results are presented, while in the latter only simulation is possible. We introduce growth and culling probabilities appropriate for condensation and evaporation on a two-dimensional surface, and compare results with existing models for this problem. Our results show a very interesting behavior under certain conditions that are quite different from earlier models. We find a possibility of hysteresis not reported earlier for such models.

DOI: 10.1103/PhysRevE.66.046104

PACS number(s): 05.10.-a, 05.70.Np, 07.05.Tp, 68.43.De

I. INTRODUCTION

The random percolation problem in two dimensions (2D) [1] can be extended to a number of interesting variations, e.g., the “bootstrapping model” [2], where certain sites are culled leading to a change in percolation behavior or the “diagenesis model” [3], with growing as well as culling. In the present model we show that an introduction of simultaneous growing and culling processes, followed by a randomization after each time step gives very interesting behavior.

The model may be applicable to a real situation such as condensation/evaporation or adsorption/desorption of a layer of “molecules” at different surface temperatures. We develop two versions of the model in subsequent sections. In model I, we assume “growth,” that is, condensation at sites where there are a large number of occupied nearest neighbors and “evaporation” at sites with most neighboring sites vacant. This algorithm mimics an attractive interaction between the molecules. We find that a certain coverage (p_{inv}) of the surface is invariant, depending on the exact algorithm employed. An initial concentration of occupied sites $p > p_{inv}$ leads to complete coverage, whereas a lower starting point $p < p_{inv}$ leads to zero coverage, i.e., complete evaporation. In Sec. II, we discuss the algorithm for growing and culling and in Sec. III a hypothetical case with a symmetric rule for activated growing and culling is discussed. In Secs. IV and V, more realistic models II and III for the condensation/evaporation process as functions of vapor pressure and surface temperature are presented. In the last section, conclusions and future plans are discussed.

II. MODEL I

We start with a square lattice in two dimensions and sites are randomly occupied by particles with a probability p . Then we grow new particles at vacancies, or cull particles at occupied sites, according to one of the rules below.

We adopt that the notation $S_i = 0$ or 1 represents vacancy or occupation of the i th site, and S_j is the same for the nearest neighbor (NN) of i . Also $n_i = \sum_j S_j$

Rule 1. (a) $n_i = \sum_{i,j}^{i \neq j} S_j$ culling: $S_i = 1$ and $n_i = 0$ or 1 lead to $S_i = 0$, i.e., occupied sites having all four NN sites vacant and occupied sites with only one NN site occupied are culled. (b) Growth: $S_i = 0$ for $n_i = 4$ or 3 leads to $S_i = 1$, i.e., a new particle grows at a vacant site with four NN positions occupied, and also at a vacant site where only three NN sites are occupied.

Rule 2. (a) Culling: $S_i = 1$ and $n_i = 0$ lead to $S_i = 1$, i.e., only particles with four vacant NN sites are culled. (b) Growth: $S_i = 0$ and $n_i = 4$, i.e., only sites with four occupied NN sites “grow” a new particle.

Rule 3. (a) Culling: $S_i = 1$ and $n_i = 0$ lead to $S_i = 1$, i.e., only particles with four vacant NN sites are culled. (b) Growth: $S_i = 0$ and $n_i = 4$ or 3, i.e., a new particle grows, at a vacant site with four NN positions occupied, and also at a vacant site where only three NN sites are occupied.

Rule 4. (a) Culling: $S_i = 1$ and $n_i = 0$ or 1, occupied sites having all four NN sites vacant and occupied sites with only one NN site occupied are culled. (b) Growth: $S_i = 0$ and $n_i = 4$, i.e., only sites with four NN sites occupied grow a new particle.

In all the above rules particles or vacant sites with two NN occupied sites are left undisturbed. Figure 1 illustrates the rules pictorially.

After completing the grow-cull operations, the concentration of particles changes from an initial value p_i to a final value p_f . We now randomize the positions of the remaining sites over the whole lattice, and repeat the grow-cull operations with p_f becoming the new p_i . The results of the above procedure for the four different rules outlined above can be determined analytically.

For each of the four rules we find an initial coverage p_{inv} , which remains invariant after repeating the steps of grow-cull operations followed by randomization. p_{inv} corresponds to the coverage for which the probability of growth equals the probability of culling for the particular rule employed.

*Email address: sujata@juphys.ernet.in

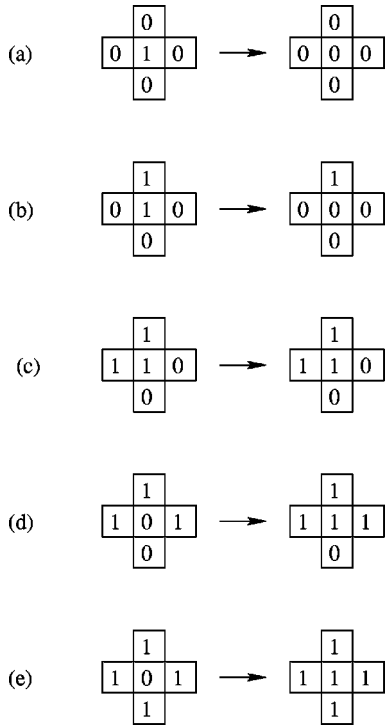


FIG. 1. The growth and culling processes are illustrated, the rules are implemented as follows: rule 1—(a), (b) (d), and (e); rule 2—(a) and (e); rule 3—(a), (d), and (e); rule 4—(a), (b), and (e).

For some other starting concentration, say $p_0 > p_{inv}$, we would get a new $p = p_1$, which is greater than p_0 , since the growth probability exceeds culling probability. The randomization that follows makes p_1 the new initial coverage, which after the grow-cull operations gives a still larger p_2 , and so on. So the coverage approaches 1.0 or 100 %, as shown in Fig. 2.

For $p_0 < p_{inv}$, on the other hand, $p_1 < p_0$ and the system evolves towards $p = 0$, i.e., zero coverage; p_{inv} is an unstable

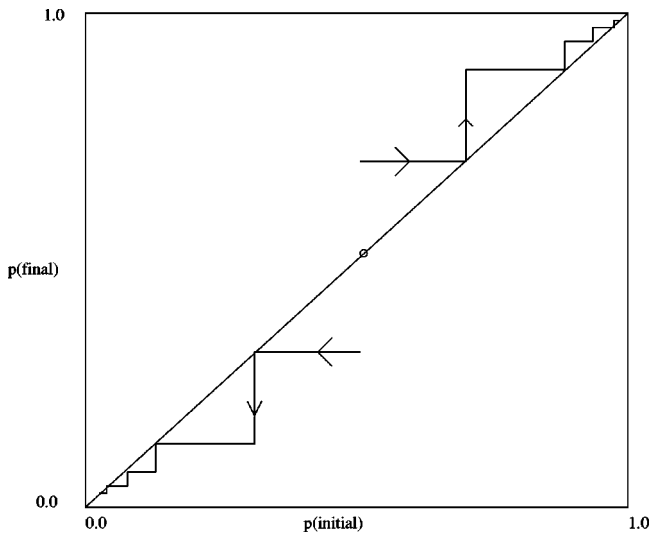


FIG. 2. This is a schematic diagram showing how the system evolves towards the fixed points, here the unstable fixed point is $p = 0.5$, valid for rules 1 and 2.

fixed point for the system, whereas $p = 0$ and $p = 1$ are stable fixed points.

The processes described above can be studied by computer simulations as well as analytically. Using a parallel algorithm for growth and culling gives a result exactly in agreement with the calculated result, while a sequential algorithm gives different results. This is explained as follows: in a sequential algorithm, one site is updated at a time according to its present surrounding. The next site, when updated, experiences an altered situation rather than the original distribution. In the parallel process one looks at all the sites and decides the updating according to the initial distribution. Then all are updated simultaneously—this is exactly equivalent to the analytical picture where the rates of growth and decay are calculated from the initial distribution.

The stable fixed point can be determined as follows. For a coverage p , the probability of growing and culling, P_{gr} and P_{cl} , for the four different rules can be written as follows. For rule 1,

$$P_{cl} = p(1-p)^4 + 4p^2(1-p)^3, \quad (1)$$

$$P_{gr} = p^4(1-p) + 4p^3(1-p)^2. \quad (2)$$

In Eq. (1) the first term on the right is the probability of an occupied site having four vacant NN sites in a random distribution. Since p is the probability of a site being occupied, and $(1-p)$ is the probability of being vacant. The other terms can be written down similarly with proper weight factors.

For the other rules, we have analogous relations. For rule 2,

$$P_{cl} = p(1-p)^4, \quad (3)$$

$$P_{gr} = p^4(1-p). \quad (4)$$

For rule 3,

$$P_{cl} = p(1-p)^4, \quad (5)$$

$$P_{gr} = p^4(1-p) + 4p^3(1-p)^2; \quad (6)$$

and for rule 4,

$$P_{cl} = p(1-p)^4 + 4p^2(1-p)^3, \quad (7)$$

$$P_{gr} = p^4(1-p). \quad (8)$$

p_{inv} is easily obtained for any of the rules by setting $P_{cl} = P_{gr}$ and solving for p .

For rules 1 and 2, which are symmetric, we find $p_{inv} = 0.5$, while for rules 3 and 4, p_{inv} has the complimentary values 0.32 and 0.68, respectively. The same values are obtained for a steady coverage by carrying out a computer simulation of the processes described by the rules.

III. ACTIVATED GROWTH AND CULLING

From physical considerations, it is expected that the probability of condensation on a surface decreases with increasing surface temperature, and probability of evaporation increases [4–6]. If we assume that rule 3 holds at high

temperatures and rule 4 at low temperature, we may introduce a hypothetical temperature-dependent growth and culling rule as follows.

$$P_{cl} = p(1-p)^4 + 4 \exp(-E_0/kT)p^2(1-p)^3, \quad (9)$$

$$P_{gr} = p^4(1-p) + 4(1 - \exp[-E_0/kT])p^3(1-p)^2. \quad (10)$$

The temperature dependence enters through the exponential factor with E_0 as an energy characteristic of the system. In fact, it is a two-state growth and culling model where a particle with one neighbor may be in one of the two states—condensed or evaporated. The probability of evaporated state is taken as $q = \exp(-E_0/kT)$ and the probability of condensed state is $(1-q)$.

The new rule can be seen to reduce to rule 3 for $T \rightarrow \infty$, and to rule 4 for $T \rightarrow 0$. The fixed point p_{inv} goes accordingly from 0.32 to 0.68 as the temperature is lowered from a very high value compared to a characteristic temperature $T_0 = E_0/k$. p_{inv} can be determined by equating the growth and culling probabilities as before at different temperatures.

The exponential temperature dependence introduced here for evaporation is realistic [4,5], but the rule for condensation is purely hypothetical, introduced to make the equation symmetric. In the following section we discuss a more realistic approach. The final coverage in this case is either 0 or 1 depending on the temperature and the initial coverage.

IV. CONDENSATION AND EVAPORATION

In this section we study the condensation/evaporation problem using the approach developed in the preceding section. We find that computer simulation of the problem is instructive, and may lead to a reinterpretation of some existing ideas.

The process of condensation/evaporation or adsorption/desorption is described traditionally by two different sets of models—one for a mobile adsorption layer and one for an immobile layer [4,5]. Probabilities for sticking and evaporation on a two-dimensional monolayer are specified according to the physics behind the model. These are functions of the temperature, the superincumbent pressure, and the existing coverage. At equilibrium, the sticking and evaporation probabilities are set equal and the resulting equation is solved to get the equilibrium coverage at that temperature and pressure.

The simplest mobile layer model is a two-dimensional ideal gas, and the improved versions include interaction between particles, similar to a two-dimensional van der Waals gas. The so-called “immobile layer” models introduce a sticking probability, depending on how long a molecule in the vapor above the surface is in contact with a surface site. The simplest ‘immobile model’ is the Langmuir equation derived as follows.

For vapor condensation the particle flux, i.e., the number of particles deposited per unit time per unit surface area is equal to

$$c = \frac{P\lambda}{h}, \quad (11)$$

where P is the pressure,

$$\lambda = \sqrt{h^2/(2\pi mkT)}$$

is the de Broglie length, and h is Planck’s constant.

Evaporation probability from saturated surface (at $p = 1$) may be approximated by [6]

$$d = \frac{kT}{h\lambda^2} \exp(-E_e/kT). \quad (12)$$

Condensation probability is set equal to the evaporation probability, giving equilibrium

$$\frac{P\lambda}{h}(1-p) = \frac{kT}{h\lambda^2} \exp(-E_e/kT)p \quad (13)$$

or

$$\frac{P\lambda^3}{kT}(1-p) = \exp(-E_e/kT)p, \quad (14)$$

and we have the simple Langmuir equation

$$Pb = \frac{p}{1-p}, \quad (15)$$

where

$$b = \frac{\lambda^3}{kT} \exp(E_e/kT),$$

E_e being the activation energy for evaporation.

In this approximation it is assumed that the evaporation energy is the same for all configurations.

A modification of this model is the Fowler-Guggenheim model [5,6]; one form of this is given below. Here the evaporation probability for a particle depends on the number of occupied neighbors. Each of the neighbors exerts an attractive force on the particle, which must be overcome for evaporation. We introduce the following parameters for convenience, f is a pressure parameter given by

$$f = P\Lambda^3/gkT,$$

$$\Lambda = \sqrt{T^*}\lambda,$$

and

$$g = \exp(-E_e/kT) = \exp(-T_0/T) = \exp(-1/T^*),$$

where $T_0 = E_e/k$ is a characteristic evaporation temperature, $T^* = T/T_0$ is a reduced temperature.

The condition for condensation rate to equal evaporation rate is now

$$f(1-p)/(T^*)^{5/2} = p^5 g^4 + 4p^4 g^3 (1-p) + 6p^3 g^2 (1-p)^2 + 4p^2 g (1-p)^3 + p(1-p)^4. \quad (16)$$

The successive terms on the right-hand side of Eq. (16) represent probabilities for a particle to have 4, 3, 2, 1, and 0 nearest neighbors in a random distribution. On rearrangement, this reduces to

$$f(1-p)/(T^*)^{5/2} = gp(1+pg-p)^4. \quad (17)$$

V. CONDENSATION/EVAPORATION FROM A DIFFERENT VIEWPOINT: MODELS II AND III

In the above models the question of mobility of the adsorption layer is not introduced explicitly, though the Fowler-Guggenheim (FG) model is classified as an immobile model. Moreover, the probabilities for evaporation considered in Eq. (16) are valid only as long as the distribution is random. For a strictly immobile layer the distribution ceases to be random once the site-dependent evaporation starts. We formulate the problem so that the lateral mobility, if present, is introduced explicitly, and we can look at both mobile and immobile situations within the same framework. As in the preceding section, we start with a two-dimensional lattice with a certain fraction occupied randomly by the particles. The adsorbate particles are also present as vapor above the surface and the pressure and temperature have a key role to play.

We visualize the condensation/evaporation (or adsorption/desorption) as a two-step process, there is one characteristic time for the sticking and evaporation and another for lateral diffusion of the molecules over the surface. For the “mobile interface” situation, the time scale for lateral motion is very small, and each condensation-evaporation step is followed by a complete randomization. The other extreme is the immobile interface, here we drop the randomization process altogether. It is also possible to consider intermediate situations where the two characteristic times are comparable.

According to this picture, setting the sticking probability equal to the evaporation probability at equilibrium is valid for the mobile situation only, not for the immobile case. This is because, if the surface molecules cannot move laterally, after one round of growth and evaporation, the expressions for condensation/evaporation probability are no longer valid, because the distribution is no longer random. So for the mobile case, we have a result similar to the Fowler-Guggenheim formalism, but with a different interpretation. Our solution for the final coverage depends on the initial coverage, besides temperature and pressure. The coverage isotherm of the system may follow a different path during increasing and decreasing pressure showing hysteresis. This mobile case, can be worked out by analytical calculation as well as computer simulation.

The immobile surface case cannot, however, be calculated analytically, as we do not know the condensation/evaporation probabilities after one round of growth and culling, since the system has lost its random distribution. But we can still simulate the system on a computer. We have two cases. First, the Fowler-Guggenheim equation in the form of Eq. (16),

which we call model II. Second, we take a situation where only particles with one occupied neighbor or none at all (isolated particles) are allowed to evaporate (as in rule 1(a), Sec. II); we call this model III. The corresponding equation is

$$f(1-p)/(T^*)^{5/2} = 4p^2(1-p)^3 + p(1-p)^4. \quad (18)$$

Temperature and pressure dependence of sticking probabilities are assigned as in the FG model, Eq. (16).

A. Mobile interface layer—analytical study

Here, there is a complete randomization after each growth-cull sequence, so it is meaningful to equate the probability of growth to the probability of culling and solve for the invariant coverage. We can look at the process as an iteration of the following two steps:

$$p_f = p_i + P_{gr} - P_{cl} \quad (19)$$

and

$$p_i = p_f, \quad (20)$$

where p_i is the initial coverage and p_f the final. Also $P_{gr} = P\lambda(1-p)/h$ and $P_{cl} = wT^{*2} \exp(-1/T^*)$. Here w is a parameter, with a suitably chosen arbitrary value. This iteration done numerically gives the same result as solving analytically,

$$P_{gr} = P_{cl}, \quad (21)$$

and also agrees with an explicit computer simulation of the process. At certain values of temperature and pressure, there are three solutions for the coverage. The middle one is an unstable fixed point (UFP), and the other two are stable fixed points. So a starting coverage above the upper fixed point leads to the coverage stabilizing at the upper fixed point, whereas if we start with a coverage below UFP we end up at the lower fixed point. The computer simulation shows exactly the same behavior. Figures 3(a) and 4(a) show the results for Eqs. (17) and (18). The difference with the standard thermodynamic treatment is as follows. If we start from a very low coverage, say at a temperature 0.5, and pressure 10^{-5} , and gradually increase the pressure, according to the earlier FG model, the coverage increases as shown in Fig. 3(a) until a phase transition to the upper fixed point takes place according to the equal area Maxwell's rule [7]. In the present model, however, stable coverage depends on initial p as well as on T^* and f . If we start with a very low p at low pressure, the system follows the same path as FG initially, but undergoes the phase transition later as shown in Fig. 3(a) (point *B*) at a pressure where the lower fixed point meets the UFP. It then follows the path *BC*. While decreasing the pressure from a higher value, the system follows the different path shown in the figure, with a phase transition where the upper fixed point coincides with UFP (point *D*). So here we have a marked hysteresis. Hysteresis in adsorption/desorption is usually attributed to the presence of pores [4], but we see here that it may also have a different origin. In

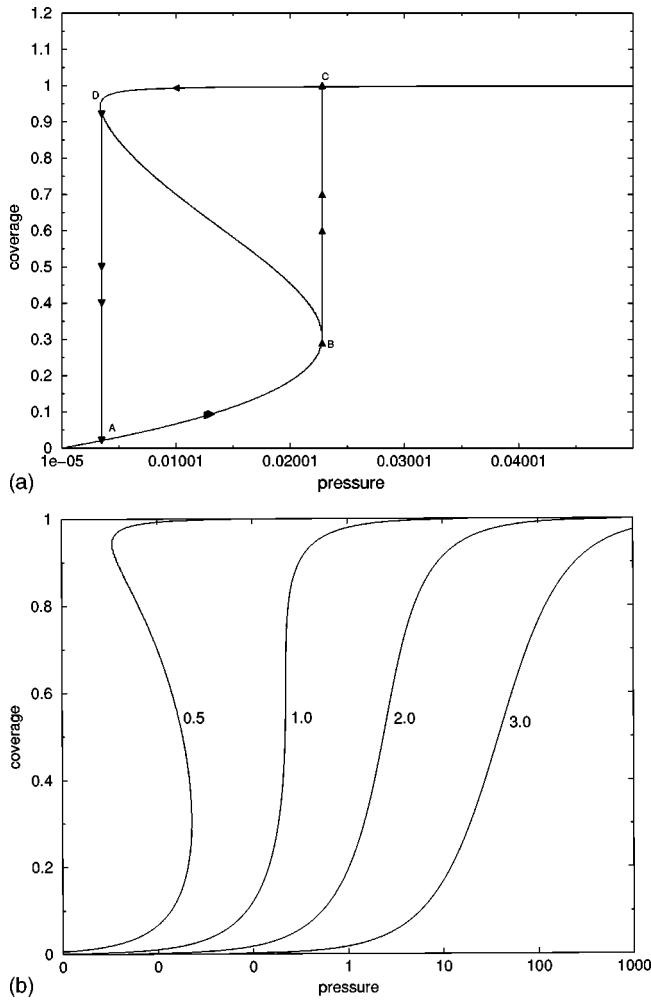


FIG. 3. (a) Coverage vs f (pressure parameter) for the mobile case (model II) with $T^* = 0.5$. If we start with a very low coverage p and gradually increase pressure, p increases along the curve upto B as shown. After this it undergoes a phase transition to $p = 1$ along BC . On decreasing pressure, it follows the path CDA showing a well-marked hysteresis. (b) Plot of final coverage vs f (pressure parameter) for different T^* .

model III [see Fig. 4(a)], the reverse path starting from high pressure and complete coverage shows no decrease in p but continues to low pressures with $p = 1$. This is because in this model there is no evaporation unless some sites are vacant. Model II looks more realistic under normal conditions. It must be noted that this is quite different from the usual form of Fowler-Guggenheim, where one would not expect hysteresis, and the present version considers a *mobile* layer.

B. Computer simulation of the mobile case

In the mobile case, the adsorbed molecules can move laterally on the surface. In model II, the physical situation simulated is described by Eq. (16). A two-dimensional square lattice of unit spacing and size 300×300 is occupied randomly with an initial coverage $p_{initial}$. Every occupied site is assigned the value of 1 and empty sites are assigned the value of 0. The occupied sites are then culled parallelly

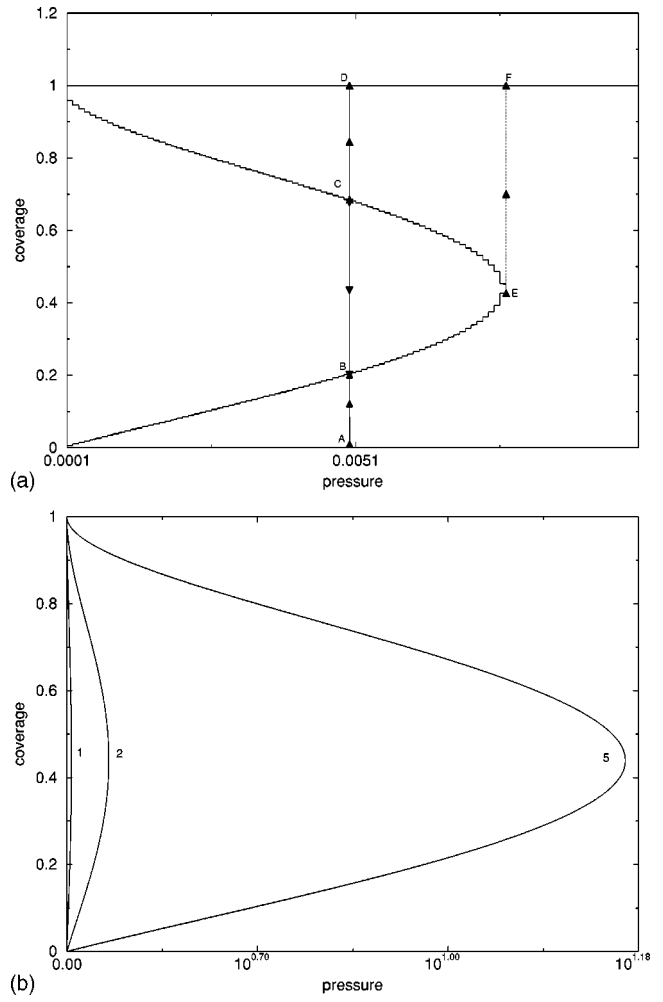


FIG. 4. (a) Plot of coverage vs f (pressure parameter) for $T^* = 0.5$ for model III. Here the final coverage depends on the initial coverage. For example, if we start at a point with coverage below B , the final coverage reaches the point B . For any starting coverage between points B and C , the final coverage is B . For starting coverage above C , the final coverage is point D ($p = 1$). Starting with a low coverage, if pressure is gradually increased, the coverage proceeds along the curve OBE , where it undergoes phase transition to F . (b) Plot of final coverage vs f (pressure parameter) for different T^* (model III).

with a probability determined by the number of their occupied nearest neighbors. The site having n occupied neighbors has the culling probability $p^{n+1}g^n$, where p is the occupation probability and

$$g = \exp(-1/T^*).$$

The vacant sites are filled with a probability $f/(T^*)^{5/2}$, where f is the pressure parameter defined earlier. After one round of growth and culling is complete, the concentration of the occupied sites p_{final} is calculated.

In the next time step, the p_{final} of the previous time step becomes the new $p_{initial}$. The square lattice is then randomly occupied afresh with this $p_{initial}$. A complete time step begins with the random occupation of all sites with a $p_{initial}$

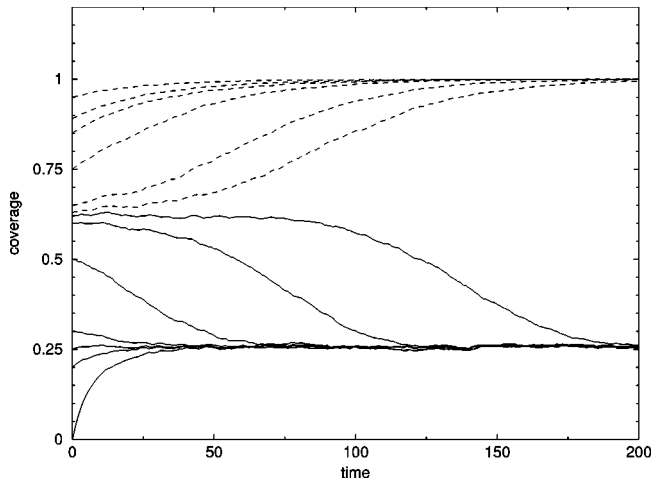


FIG. 5. Plot of coverage vs time steps for the mobile case. For initial coverages above 0.68 (dotted lines), the final coverage is $p = 1$. For coverages below 0.68 (solid lines), the final p is the lower fixed point.

and ends with the assignment of the p_{final} to the $p_{initial}$ of the next time step. This iterative process stops when $p_{final} = 0$ or 1 or p_{final} saturates with increasing time to a definite value. In the simulation, we checked upto 50 000 time steps. The mobility of the molecules is simulated by the randomization of the concentration $p_{initial}$ in the beginning of every time step.

In model III described by Eq. (18), the same iterative process described in model II is carried out, except for the condition of culling. In this case, an occupied site is culled with the probability g if the sum of its nearest neighbors is less than 2.

All the sites in both the models are updated parallelly and periodic boundary conditions are applied both along the x and y directions. Both the models are studied over an effective temperature range of 0.5–3 and with f varying from 10^{-4} to 10^2 for the entire range of $p_{initial}$ from 0 to 1. The simulation results agree to within 10^{-3} of the numerical results. These are presented in the Figs. 3(a), 3(b), 4(a), 4(b), and 5).

A significant difference between models II and III is evident from Figs. 3(b) and 4(b), showing isotherms for different temperatures. In model II there is a critical temperature above which there is no phase transition, but in model III there is always a phase transition. Figure 5 shows how the coverage evolves with time for $T^* = 0.5$ and $f = 0.02$ for $p_{initial}$ varying from 0 to 1.

C. Immobile interface layer

Let us now make the adsorbed molecules immobile. In this case obviously, analytical calculation is not feasible. If we start with an initial random configuration with a certain coverage, as soon growth and culling at preferential locations starts we can no longer calculate probabilities for further evolution exactly. So here we resort to computer simulation. The simulation of the immobile case of the models II and III follow the same iterative process, except for the randomiza-

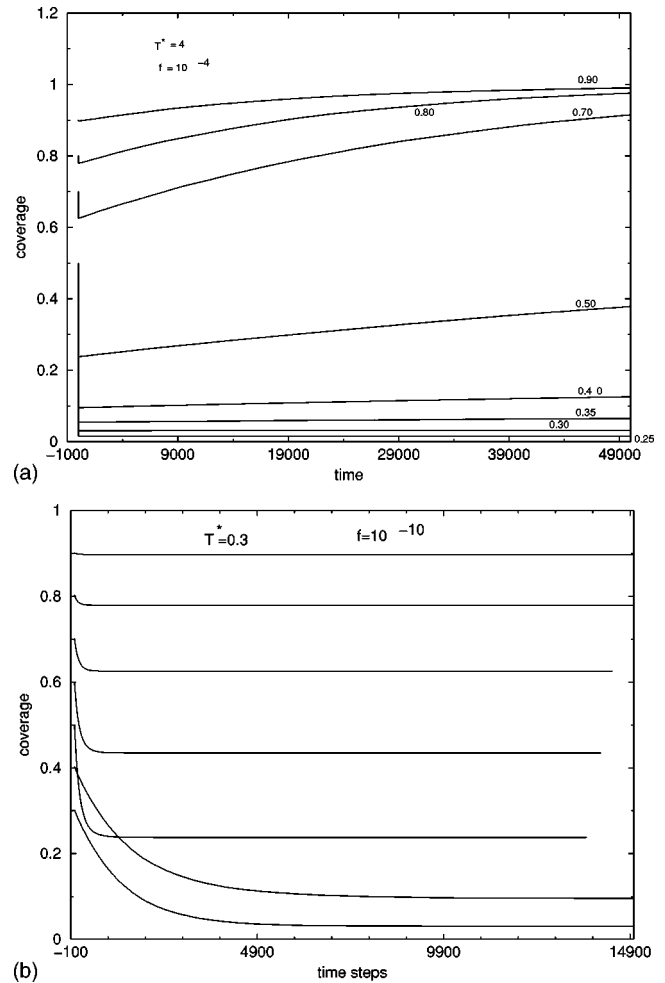


FIG. 6. (a) Plot of coverage vs time steps for the immobile case in model III for $T^* = 4$ and $f = 10^{-4}$. For initial coverage below 0.35, the final coverage saturates to different values. But for larger initial coverage, the system approaches $p = 1$. The numbers on the curves indicate the initial coverage. The y axis is shifted from $t = 0$ to show clearly the initial drop of the coverage at early times. (b) Plot of coverage vs time steps for the immobile case in model III for $T^* = 0.3$ and $f = 10^{-10}$. Here the final coverage saturates to different values for all the initial coverages studied over 50 000 time steps.

tion of the sites with the given probability at the beginning of every time step. Here a new round of growth and culling commences on the geometrical configuration reached at the end of the last time step. Since in the preceding section, we saw that computer simulation results agree with calculations, we are confident that the simulation gives reliable results, with the system size and algorithm used.

We find that the results are quite different from the *mobile* case. Whereas in the mobile case we found definite fixed points where the coverage converged regardless of the exact starting p (see Fig. 5), here, for certain ranges of the temperature and pressure parameters, we get a different stable coverage for even closely spaced initial p values. Figures 6(a) and 6(b) show the time evolution of the coverage for the immobile system for typical situations under quite different conditions of pressure. In Fig. 6(a), for $p_{initial}$ above 0.3, the

coverage always goes to 1 at rates depending on the initial coverage, but for lower starting points it stabilizes to different values for each $p_{initial}$. In a similar study of the *mobile* case, one always ends up at either the upper or the lower fixed point (Fig. 5). But Fig. 6(a) shows that for the *immobile* case, initially culling dominates, for large $p_{initial}$ there is a rapid drop in coverage within a few hundred time steps. After that sticking catches up, and for $p > 0.3$ (approximately) there is a steady increase, and $p \rightarrow 1$ linearly with a slope decreasing as $p_{initial}$ decreases. For $p_{initial}$ lower than ~ 0.3 , p apparently saturates, showing no variation upto 50 000 time steps. But when the same situation is studied at a much lower $f(10^{-10})$, [Fig. 6(b)], p_{final} always saturates to different values depending on $p_{initial}$, over the time scales checked. For example, in Fig. 6(a), for $p_{initial} = 0.9$, $p_{final} = 1$ whereas the same $p_{initial}$ in Fig. 6(b), saturates to p_{final} of 0.8979. This suggests that even for the same $p_{initial}$, there must be a definite combination of pressure and temperature where there is a change in the behavior— p_{final} reaching the stable fixed point 1 or a constant value of < 1 . Further investigations probing the exact phase diagram are in order and will be done in the near future.

All the above figures are the results using model III. Similar studies on model II show no significant qualitative difference with model III except for the exact numerical values.

VI. CONCLUSIONS

We have investigated the behavior of a two-dimensional surface layer explicitly allowing or forbidding lateral motion of the particles. We find that the cases for a mobile and an immobile layer show quite different characteristics, moreover, none agrees fully with the Langmuir or FG model. The fixed points for our model II with mobile particles are the same as the FG solutions, which are supposed to be valid for an *immobile layer*. Details of the evolution of the surface coverage from low to high pressure are, however, different. For the immobile layer the results are again different. These results are similar to what was reported in a previous work

attempting to simulate diagenetic processes of restructuring in sandstones [3]. However, the two-dimensional character is more appropriate in case of the condensation/evaporation problem. It will be interesting if experimental support for the behavior described here can be demonstrated. Hysteresis has been observed for adsorption on porous surfaces [4], but here we see that competition between site-specific sticking and evaporation may also cause hysteresis.

We can simulate intermediate behavior between mobile and immobile layers, by allowing the particles to execute a random walk for some time on the surface before the next grow-cull operation. Making the time for the walk extremely large will correspond to the complete randomization done here. We have plans to study this in future.

Recent work on adsorption/desorption problems [8–13] show that considerable theoretical and experimental studies are being done on such problems. They are of interest in modern devices that use surface properties extensively, and are also useful for environment related problems such as explaining the ozone hole in polar regions [4,9]. Complicated mathematical and computer simulation methods such as density functional theory and molecular dynamics simulations are being used. In this work we show that very simple Monte Carlo simulations also reveal some interesting features and may turn out to be quite useful in shedding some light on such problems. In conclusion the growth-culling-randomization extension of the standard 2D percolation problem promises to yield more new and interesting results.

ACKNOWLEDGMENTS

The DST, the Government of India, and the Ministry of Ukraine for Education and Science are gratefully acknowledged for the grant of an Indo-Ukrainian collaboration project. The authors thank S. S. Manna and J. K. Bhattacharjee for suggestions and discussion on this subject. The authors are grateful to the S. N. Bose National Center for Basic Sciences for extending to us the use of their computer facilities.

-
- [1] D. Stauffer and A. Aharony, *Introduction to Percolation Theory* (Taylor & Francis, London, 1994).
 - [2] S. S. Manna, *Physica A* **261**, 351 (1998).
 - [3] S. S. Manna, T. Datta, R. Karmakar, and S. Tarafdar, *Int. J. Mod. Phys. C* **13**, 319 (2002).
 - [4] E. M. McCash, *Surface Chemistry* (Oxford University Press, New York, 2001).
 - [5] S. Ross and J. P. Olivier, *On Physical Adsorption* (Interscience/Wiley, New York, 1964).
 - [6] M. J. Jaycock and G. D. Parfitt, *Chemistry of Interfaces* (Wiley, Chichester, 1981).
 - [7] K. Huang, *Statistical Mechanics* (Wiley, New York, 1963).
 - [8] P. Gupta, P. A. Coon, B. G. Koehler, and S. M. George, *J. Chem. Phys.* **93**, 2827 (1990).
 - [9] D. R. Haynes, N. J. Tro, and S. M. George, *J. Phys. Chem.* **96**, 8502 (1992).
 - [10] J. Toth, *Adv. Colloid Interface Sci.* **55**, 1 (1995).
 - [11] K. Sing, *Colloids Surf., A* **187-188**, 3 (2001).
 - [12] A. Dabrowski, *Adv. Colloid Interface Sci.* **93**, 135 (2001).
 - [13] W. Steele, *Appl. Surf. Sci.* (to be published).